

# Nuclear Accretion in Galaxies of the Local Universe: Clues from *Chandra* Observations

S. Pellegrini

*Astronomy Department, Bologna University, Italy;*  
*silvia.pellegrini@unibo.it*

ApJ in press; received Nov. 5, 2004, accepted Jan. 28, 2005

## ABSTRACT

In order to find an explanation for the radiative quiescence of supermassive black holes in the local Universe, for a sample of nearby galaxies the most accurate estimates are collected for the mass of a central black hole ( $M_{BH}$ ), the nuclear X-ray luminosity  $L_{X,nuc}$  and the circumnuclear hot gas density and temperature, by using *Chandra* data.  $L_{X,nuc}$  varies by  $\sim 3$  orders of magnitude and does not show a relationship with  $M_{BH}$  or with the Bondi mass accretion rate  $\dot{M}_B$ .  $L_{X,nuc}$  is always much lower than expected if  $\dot{M}_B$  ends in a standard accretion disc with high radiative efficiency (this instead can be the case of the active nucleus of Cen A). Radiatively inefficient accretion as in the standard ADAF modeling may explain the low luminosities of a few cases; for others, the predicted luminosity is still too high and, in terms of Eddington-scaled quantities, it is increasingly higher than observed, for increasing  $\dot{M}_B$ . Variants of the simple radiatively inefficient scenario including outflow and convection may reproduce the low emission levels observed, since the amount of matter actually accreted is reduced considerably. However, the most promising scenario includes feedback from accretion on the surrounding gas: this has the important advantages of naturally explaining the observed lack of relationship between  $L_{X,nuc}$ ,  $M_{BH}$  and  $\dot{M}_B$ , and of evading the problem of the fate of the material accumulating in the central galactic regions over cosmological times.

*Subject headings:* accretion, accretion disks — galaxies: elliptical and lenticular, cD — galaxies: nuclei — X-rays: galaxies

## 1. Introduction

Improved ground based instrumentation and especially the use of *HST* have shown a widespread presence of central dark objects of  $10^7 - 10^9 M_\odot$ , most likely supermassive

black holes (SMBHs), at the center of spheroids (bulges and early-type galaxies) in the local Universe (Magorrian et al. 1998, van der Marel 1999, Gebhardt et al. 2003). A possible relationship between these galaxies and the relics of the “quasar era” has therefore been suggested (Richstone et al. 1998, Yu and Tremaine 2002). Most nearby nuclei, though, are radiatively quiescent or exhibit low levels of activity. For example, in terms of the Eddington luminosity, while  $L/L_{Edd} \sim 1$  in powerful AGNs,  $L/L_{Edd} \sim 10^{-9}$  in SgrA\* (Yuan et al. 2003) that hosts a securely measured SMBH mass, and  $L/L_{Edd} < 10^{-8}$  in the nearby elliptical galaxies NGC1399, 4636 and 4472 (Loewenstein et al. 2001). In the statistically complete spectroscopic survey of galaxies with  $B_T < 12.5$  mag (Ho et al. 1997) only  $\sim 40\%$  of the nuclei show line emission that could be explained by accretion. This radiative quiescence represents one of the most intriguing aspects of SMBHs in the local Universe (as already recognized by Fabian and Canizares 1988). At the same time, correlations have been discovered involving the SMBH masses ( $M_{BH}$ ) and global properties of their host galaxies, as the central stellar velocity dispersion  $\sigma$  (Gebhardt et al. 2000, Ferrarese and Merritt 2000). These observational facts have led to think that the birth, growth and activity cycle of SMBHs and the evolution of their host galaxies are tightly linked. However, it is still under study how the tight correlations were established, whether the radiative quiescence is linked to the mechanism responsible for the  $M_{BH} - \sigma$  relation, and why and how the luminous AGNs switched off (e.g., Haiman et al. 2003).

In this work the question of why local SMBHs are not bright is addressed. The answer is not in a different value for  $M_{BH}$ , since the respective SMBH masses of distant AGNs and local nuclei cover roughly the same range (Ho 2002). It could then reside in a low mass accretion rate  $\dot{M}$ , or in a low radiative efficiency, or in the existence of activity cycles. The most promising solution among these is here looked for by collecting three quantities that play a fundamental role in this problem (the nuclear emission,  $M_{BH}$  and  $\dot{M}$ ) for a sample of galactic nuclei in the local Universe, and by searching for possible relationships among them. This is accomplished by using *Chandra* results for the galactic nuclei and the best estimates available of their  $M_{BH}$ . With the *Chandra*  $\sim 0''.3$  FWHM PSF (Van Speybroeck et al. 1997) it has become possible to get a clean look at the faint nuclear emission that may be associated with SMBHs and also at the hot gas properties close to the accretion radius, where the dynamics of the gas start to be dominated by the potential of the SMBH. This allows us to estimate  $\dot{M}$  in the simplest case of the steady and spherically symmetrical Bondi (1952) solution ( $\dot{M}_B$ ). A mass accretion rate of the order of  $\dot{M}_B$  enters also in the viscous rotating analog of the Bondi treatment represented by radiatively inefficient accretion flow models (Narayan and Yi 1995, Quataert 2003).

In sect. 2 the collected sample is presented, spanning morphological types from E to Sbc. In Sect. 3 the mass accretion rate  $\dot{M}_B$  is derived in a homogeneous way for a sub-

sample of early-type galaxies, and the possible sources of uncertainty are discussed; then, the relationship between  $L_{X,nuc}$ ,  $M_{BH}$  and  $\dot{M}_B$  are investigated. In Sect. 4 the observational findings are summarized and compared with the predictions of various models for low luminosity accretion. In Sect. 5 the results are discussed further.

## 2. The sample

For this study all nearby nuclei with a Chandra investigation of their nuclear luminosity  $L_{X,nuc}$  are considered. A few nuclei classified as Seyfert (Ho et al. 1997), or residing in peculiar objects as starburst and closely interacting systems, or with a highly uncertain  $L_{X,nuc}$  estimate (e.g., due to severe pile-up problems) have been excluded. The elliptical Cen A, the nearest active galaxy, is added to the sample for comparison and later reference. In order for a nucleus to be included, its  $M_{BH}$  estimate must derive from specific modeling (e.g., Gebhardt et al. 2003 for NGC4697) or it must be possible to calculate it from the  $M_{BH} - \sigma$  relation of Tremaine et al. (2002), for the proper  $\sigma$  value [this is derived from McElroy (1995) or the HyperLeda catalogue]. The  $M_{BH} - \sigma$  relation has an intrinsic dispersion in  $M_{BH}$  within a factor of two (Tremaine et al. 2002). The resulting 50 host galaxies are listed in Table 1; their morphological types go from E0 to Sbc (as shown by Fig. 1 discussed in Sect. 3.1). The circumnuclear hot gas density  $\rho$  and temperature  $T$  have been derived from a *Chandra* pointing for 17 of the galaxies in Table 1, in addition to the Galactic Center. All these are early-type systems: 15 are E or S0 galaxies, 2 of them are Sa (Sombrero and NGC1291).

Since distance-dependent quantities are involved in this work, distances obtained in a homogeneous way have been adopted (column 2), as are those derived from the SBF method by Tonry et al. (2001); this is possible for most of the galaxies, for the others (labeled in Tab. 1) the adopted distance refers to  $H_0 = 75 \text{ km s}^{-1} \text{ Mpc}^{-1}$ , a value consistent with the  $H_0$  implied by Tonry et al. (2001). The values of  $T$ ,  $\rho$  and  $L_{X,nuc}$  in columns 5, 6, and 7 have been derived by the authors referenced in column 8, and have been rescaled for the distance in column 2 when necessary. The values of  $M_{BH}$  in column 3 have been rescaled for the distance in column 2 when needed; the source of the  $M_{BH}$  estimate is given in column 4.

$L_{X,nuc}$  is that of a point source located at the optical or radio center of the galaxy. In most cases, the nuclear emission is hard and its spectral distribution can be modeled with a power law of photon index  $\Gamma = 1 - 2$ . The uncertainty on  $L_{X,nuc}$  is typically well within 20%; in 11 cases just an upper limit could be placed on  $L_{X,nuc}$ . The values of  $\rho$  and  $T$  in Tab. 1 refer to the accretion radius  $r_{acc} = 2GM_{BH}/c_s(\infty)^2$ , where  $c_s(\infty)$  is a “fiducial” sound speed of the ISM [i.e., valid in the circumnuclear region; see eq. (2.38) of Frank et al.

2002]. At  $r_{acc}$  the ratio of internal energy to gravitational binding energy of a gas element is  $\sim 1$  and therefore for  $r \lesssim r_{acc}$  the gravitational pull of the SMBH is the prevailing force on the surrounding ISM (if heating sources can be neglected). For the selection of nuclei with  $\rho$  and  $T$ , a distance limit of 50 Mpc has been adopted, in order for the *Chandra* ACIS angular resolution to provide a reasonable measurement (a typical  $r_{acc}$  of 100 pc corresponds to 0.4 arcsec at 50 Mpc). In this way the  $\rho$  and  $T$  values in Tab. 1 have been directly estimated at or extrapolated reasonably well to their  $r_{acc}$  (whose angular size ranges from 0".2 to 2"), by deprojection of X-ray imaging and spectroscopic data. For four galaxies in Tab. 1, instead, they are an average over a central region whose radius is much larger than  $r_{acc}$  (M32, NGC821, NGC1553 and NGC4438)<sup>1</sup>. How are these  $\rho$  and  $T$  likely to vary if calculated at  $r_{acc}$ ? In the cases studied best with *Chandra*,  $T$  does not vary more than 50% in the central galactic region, being usually decreasing towards the center (see, e.g., Di Matteo et al. 2003 for M87, Kim and Fabbiano 2003 for NGC1316, Ohto et al. 2003 for NGC4636); the radial density distribution, instead, always raises smoothly down to the smallest observed radii, with an increase by a factor of a few or more. The effect of this uncertainty for these four galaxies is taken into account when  $\rho$  and  $T$  are used below (Sects. 3.2–3.4).

### 3. Results

#### 3.1. $L_{X,nuc}$ and $M_{BH}$

The relationship between the nuclear X-ray luminosity and the SMBH mass is shown in Fig. 1. No clear trend between these two quantities is apparent from this plot. A lack of nuclei with high  $L_{X,nuc}$  and  $M_{BH}$  between 1 and  $5 \times 10^7 M_{\odot}$  can be seen, but its real existence should be further checked with larger samples when available. On the contrary it is clear that, for  $M_{BH} > 5 \times 10^7 M_{\odot}$ ,  $L_{X,nuc}$  varies by a large factor, roughly three orders of magnitude, at any fixed  $M_{BH}$ .

The nucleus with the highest  $L_{X,nuc}$  in Fig. 1 is that of the active galaxy Cen A (see Tab. 1). Excluded Cen A, the six brightest nuclei are those of NGC3169, NGC3226, NGC4261, NGC4486, IC1459, IC4296. From their optical emission line spectra, these are classified as LINERs or show weak or absent optical lines (Ho et al. 1997, Phillips et al. 1986, Wills et al. 2002). The last four of these are also radio galaxies, the first two are not. Note that

---

<sup>1</sup>For example, for M32 they refer to an annulus of radii of 15" and 44", they are an average over a central region of projected radius of 20" for NGC821, and an average over a central spiral-like region extending  $\sim 30''$  for NGC1553 (see the references in column 8).

there are other radio galaxies in Fig. 1 (e.g., NGC1316 and NGC4374) that instead have  $L_{X,nuc} < 10^{40}$  erg s $^{-1}$ . In this respect it is interesting to note that the core radio luminosity of nearby galactic nuclei shows a similar large variation and lack of relation with the SMBH mass for  $M_{BH} \sim 10^7 - 10^9 M_{\odot}$  (Ho 2002).

### 3.2. $L_{X,nuc}$ and $\dot{M}_B$

The next interesting relationship to investigate is that between the nuclear luminosity and the mass potentially available for accretion. This makes use of  $\rho$  and  $T$  collected in Table 1. The simplest assumption to make is that gas accretion is steady and spherically symmetric as in the standard theory developed for gas accreting onto a point mass at rest with respect to it (Bondi 1952). In this theory the accretion rate  $\dot{M}_B$  is given by [see eq. (2.36) of Frank et al. 2002]

$$\dot{M}_B = \pi G^2 M_{BH}^2 \frac{\rho(\infty)}{c_s^3(\infty)} \left[ \frac{2}{5 - 3\gamma} \right]^{(5-3\gamma)/2(\gamma-1)} \quad (1)$$

where  $\gamma$  is the polytropic index that varies from 1, in the isothermal case, to 5/3 in the adiabatic case;  $c_s = \sqrt{\gamma kT/\mu m_p}$  is the sound speed of the gas, with  $m_p$  the proton mass and  $\mu$  the mean mass per particle of gas measured in units of  $m_p$ ;  $\mu$  is assumed here to be equal to 0.62, corresponding to a solar chemical composition; finally, “ $\infty$ ” refers to the ambient conditions. It is usually assumed that the accretion rate is determined by  $\rho$  and  $T$  at the radius where the influence of the black hole becomes dominant (i.e., close to  $r_{acc}$  defined in Sect. 2). The relationship between  $L_{X,nuc}$  and  $\dot{M}_B$  is shown in Fig. 2, for  $\gamma = 1.33$  (an intermediate value between the two limits). For the cases where  $\rho$  is likely an underestimate of  $\rho(r_{acc})$  and  $T$  could overestimate  $T(r_{acc})$  (as discussed at the end of Sect. 2),  $\dot{M}_B$  derived here is likely an underestimate of the true  $\dot{M}_B$  [from eq. (1)] and as such is marked in Fig. 2. No clear trend between  $L_{X,nuc}$  and  $\dot{M}_B$  is shown by Fig. 2; a scatter of  $\sim 3$  orders of magnitude is shown by both  $L_{X,nuc}$  and  $\dot{M}_B$ .

For a few of the nuclei in Fig. 2 a “Bondi mass accretion rate” had already been calculated by the authors referenced in Table 1 (col. 8), by using though slightly different definitions for  $\dot{M}_B$ , different ways of estimating  $M_{BH}$  and the gas density  $\rho$  to be inserted in eq. (1) from observational data, different values for  $\gamma$  and  $\mu$ , and distances derived with different methods and not referring to the same distance scale. A re-calculation of  $\dot{M}_B$  in a homogeneous way was needed here in order to consider the problem of the nature of accretion for these nuclei as a class. Unfortunately, residual uncertainties remain on the  $\dot{M}_B$  derived here. From eq. (1), they are due to the errors on the estimate of  $\rho(r_{acc})$ ,  $T(r_{acc})$  and  $M_{BH}$ ;

in addition, the possible range of values for  $\gamma$  between 1 and 5/3 causes  $\dot{M}_B$  to vary by a factor of 9.68. The size of the uncertainty on  $\dot{M}_B$  can be estimated accurately for 7 galaxies for which errors on  $\rho$  and  $T$  in Tab. 1 are given in the literature, by using the standard error propagation formula. The results are shown in Figs. 2 and 3. Cen A and Sombrero have the largest uncertainties on  $\dot{M}_B$ , due to the error on the respective  $M_{BH}$  values.

### 3.3. $L_{X,nuc}$ and $L_{acc}$

If at very small radius the accreting gas  $\dot{M}_B$  joins a standard accretion disc (Shakura and Sunyaev 1973), so that the final stages of accretion are similar to those of bright AGNs, an accretion luminosity  $L_{acc} \sim 0.1\dot{M}_B c^2$  is expected. This is plotted as a solid line in Fig. 2. All the nuclei lie well below this expectation, which is a representation of the underluminosity problem for nearby galactic nuclei with the presently best available data. On the contrary, the nucleus of Cen A (recognizable by its highest  $L_{X,nuc}$  value in Fig. 2) could host a standard disc with an accretion rate close to  $\dot{M}_B$ . Note that the bolometric luminosity  $L_{bol}$  of the nuclei should be used for a comparison with  $L_{acc}$ ; however, even when considering  $L_{bol}$  instead of  $L_{X,nuc}$ , the conclusions are likely to remain unchanged. For example, the canonical bolometric correction for AGNs is  $L_{bol}/L_X \sim 10$  (Elvis et al. 1994); more specifically for the nuclei of NGC4261, NGC4594 and M87 (three galaxies in Table 1) the ratio  $L_{bol}/L_{0.5-10\text{keV}}$  is respectively 14, 8 and 17, calculated from their whole spectral energy distributions (Ho 1999). These values do not fix the underluminosity problem.

### 3.4. Relationship between Eddington-scaled quantities

Fig. 3 shows the relationship between the Eddington-scaled quantities  $L_{X,nuc}/L_{Edd}$  and  $\dot{M}_B/\dot{M}_{Edd}$  (with  $\dot{M}_{Edd} = L_{Edd}/0.1c^2$ ). The reason for plotting Eddington-scaled quantities lies in the possibility of a direct comparison with the predictions of low radiative efficiency accretion flows (ADAF, Narayan and Yi 1995). These can develop in the conditions of very low  $\dot{m}$  (defined as  $\dot{m} = \dot{M}/\dot{M}_{Edd}$ ), precisely when  $\dot{m} < \alpha^2 \lesssim 0.1$ , where  $\alpha$  is a viscosity parameter for the flow. ADAF models predict a rate of mass accretion  $\dot{M}$  comparable to the Bondi rate, with a more accurate estimate that may be  $\dot{M} \approx \alpha\dot{M}_B$  (Quataert 2003). Given the values of the abscissae for the points in Fig. 3, these nuclei are candidate to host ADAFs. In these flows the matter is so hot and tenuous that it is unable to radiate strongly; most of the gravitational potential energy is advected by ions inside the event horizon. The ADAF

emission is in the X-ray and in the radio bands<sup>2</sup>, and scales as  $L_{ADAF} \sim 0.1\dot{M}c^2(\dot{m}/\alpha^2)$  (Narayan and Yi 1995). This emission level is plotted in Fig. 3 as a dashed line, for the two cases of  $\dot{M} = \dot{M}_B$  and  $\dot{M} = \alpha\dot{M}_B$ , with  $\alpha = 0.1$  (a value typically assumed for galactic SMBHs, Di Matteo et al. 2003). Fig. 3 shows that  $L_{ADAF}$  is in fact much lower than  $L_{acc}$ , so that an ADAF may explain the emission level for a few nearby galactic nuclei. However,  $L_{ADAF}$  is still too high for the emission level of many other nuclei. The most discrepant cases are those of the galaxies in the lower right portion of Fig. 3, that are NGC4472 and NGC1399 (see also Loewenstein et al. 2001), NGC4649 and the Galactic Center (e.g., Baganoff et al. 2003, Yuan et al. 2003). Note also how the possibility for an ADAF to reproduce the observed values of  $L_{X,nuc}$  decreases with increasing  $\dot{M}_B/\dot{M}_{Edd}$ , since  $L_{ADAF}/L_{Edd}$  increases steeply as  $\dot{m}^2$ .

#### 4. Summary

For a sample of galaxies of the local Universe that excludes Seyferts, starbursts and peculiar objects, the most accurate estimates available for  $M_{BH}$ ,  $L_{X,nuc}$  and circumnuclear  $\rho$ ,  $T$  have been collected, with the aim of studying possible relationships between  $M_{BH}$ ,  $L_{X,nuc}$  and the Bondi mass accretion rate  $\dot{M}_B$ . It is found that:

- $L_{X,nuc}$  does not show a relationship with  $M_{BH}$ . It exhibits a large scatter, up to  $\sim 3$  orders of magnitude, for any fixed  $M_{BH} > 5 \times 10^7 M_\odot$ . Note that the core *radio* luminosity of nearby galactic nuclei shows a similar large variation and lack of relation with the SMBH mass, for  $M_{BH} \sim 10^7 - 10^9 M_\odot$  (Ho 2002).
- $L_{X,nuc}$  does not show a relationship with  $\dot{M}_B$  either, even though the uncertainties in the latter may be large.  $\dot{M}_B$  also spans a range of  $\sim 3$  orders of magnitude. The emission level given by  $L_{acc} \sim 0.1\dot{M}_Bc^2$ , describing the expected emission if  $\dot{M}_B$  ends in a standard accretion disc, is much larger than the observed  $L_{X,nuc}$  values. Therefore in general, as long as  $\dot{M}_B$  is a good estimate of the true mass accretion rate  $\dot{M}$ , the nuclei are not downsized AGNs, in the sense that their low level of emission cannot be accounted for just by a  $\dot{M} \ll \dot{M}_{Edd}$ .
- radiatively inefficient accretion as in the standard ADAF modeling may explain the low luminosities of some nuclei; for others, the predicted emission level is still higher than observed. In addition, the ADAF-predicted luminosity is increasingly higher than the lowest  $L_{X,nuc}$  observed, for increasing  $\dot{M}_B/\dot{M}_{Edd}$ .

---

<sup>2</sup>The radio emission from an ADAF scales with the SMBH mass and the X-ray luminosity as  $L_{15\text{GHz}} \sim 10^{36}(M_{BH}/10^7M_\odot)(L_{2-10\text{keV}}/10^{40}\text{erg s}^{-1})^{0.14} \text{ erg s}^{-1}$  (Yi and Boughn 1999).

Radiatively inefficient scenarios include also ‘advection dominated inflow/outflow solutions’ (ADIOS, Blandford and Begelman 1999) and ‘convection dominated accretion flows’ (CDAFs, Quataert and Gruzinov 2000, Igumenshchev et al. 2000), where much less than the mass available at large radii (i.e., of  $\dot{M}_B$ ) is actually accreted on the SMBH. ADIOS prevent accretion by removing completely some of the inflowing matter via a polar outflow, in CDAFs accretion is stalled by convecting the material back out to larger radii. The accretion of rotating gas may also result in a reduced  $\dot{M}$  relative to the Bondi rate (Proga and Begelman 2003). All these variants of the simple radiatively inefficient scenario may be able to reproduce the low emission levels observed, by reducing considerably the amount of matter that is actually accreted.

However, the observational evidence of the independence of  $L_{X,nuc}$  from  $M_{BH}$  and  $\dot{M}_B$  provided by Figs. 1, 2 and 3 is best explained if there is feedback from the SMBH accretion on the surrounding ISM. Feedback can be provided by radiative or momentum driven heating of the circumnuclear gas. In this scenario accretion undergoes activity cycles: while active, the central engine heats the surrounding ISM, so that accretion is offset; then the ISM starts cooling again and accretion resumes. Intermittent accretion was already suggested and investigated in the context of the evolution of galactic cooling flows, and proposed heating sources were the nuclear hard radiation (Ciotti and Ostriker 2001) or the deposition of the mechanical energy of nuclear outflows (Binney and Tabor 1995, Omma et al. 2004). Also in the case of ADIOS the predicted wind may have an impact on the hot gas at large scales, although this aspect has not been addressed in detail yet. The intermittent accretion scenario could then be described by a series of ADIOS with time dependent outer boundary conditions (e.g., Yuan et al. 2000).

If there is feedback, and accretion becomes intermittent, the estimate of  $\dot{M}$  given by a steady spherically symmetric theory without heating sources, such as the Bondi theory, may be misleading. Also, no clear relationship of  $L_{X,nuc}$  with  $\dot{M}_B$  and  $M_{BH}$  is expected. In a plot like Fig. 2 Cen A could be accreting at the present time with  $\dot{M} \sim \dot{M}_B$  and with a high radiative efficiency; the bulk of the nuclei would be accreting with a largely different  $\dot{M}$ , since they are captured in various stages of their complex evolution. Nearby early-type galaxies for which a search for nuclear emission has been made using the *Chandra* data, but no detection was found, together with a few of the upper limits on  $L_{X,nuc}$ , may correspond to truly inactive SMBHs, where accretion is temporally switched off due to feedback.



## 5. Discussion

Other, more indirect, arguments favoring a role for feedback are discussed in this last Section.

In favor of the existence of activity cycles is some observational evidence coming from a galactic scale, where *Chandra* revealed hot gas disturbances that are reconducted to the effects of recent nuclear activity. For example two symmetric arm-like features cross the center of NGC4636 (Jones et al. 2002), and are accompanied by a temperature increase with respect to the surrounding hot ISM; they were related to shock heating of the ISM, caused by a recent nuclear outburst. A similar hot filament crosses the nuclear region of NGC821 (Fabbiano et al. 2004) and a nuclear outflow has been detected in NGC4438 (Machacek et al. 2004). Cavities and surface brightness edges related to radio activity have been revealed in NGC4374 (Finoguenov and Jones 2001) and NGC4472 (Biller et al. 2004).

On the other hand the possibility that radiatively inefficient accretion takes place after the end of the bright QSO phase for cosmological times seems problematic. If accretion at an average rate (from Fig. 2) of  $\dot{M} \sim 10^{-2} M_{\odot}\text{yr}^{-1}$  steadily accumulates mass at the galactic centers for  $\sim 10$  Gyrs, then SMBH masses of  $\sim 10^8 M_{\odot}$  are formed. SMBHs of masses  $M_{BH} \gtrsim 10^8 M_{\odot}$  already come from accretion with high radiative efficiency during the optically bright QSO phase (Yu and Tremaine 2002), therefore after the end of this phase SMBH growth by accretion with low radiative efficiency at the  $\dot{M}_B$  of Fig. 2 cannot have been very important. Solutions as ADIOS and CDAF predict an effective  $\dot{M}$  much lower than  $\dot{M}_B$ ; in this case, however, it is unclear where does the gas that fails to accrete go, whether it accumulates in the circumnuclear region and for how long these solutions can prevent mass from accreting. On the contrary, feedback modulated accretion has the possibility of displacing gas far from the galactic center and even removing it from the galaxy; therefore it presents the advantage of accumulating much less mass at the galactic centers (e.g., Ciotti and Ostriker 2001). The low radiative efficiency solutions could however represent a temporary effect, for example taking place within an intermittent accretion scenario, or considering that the circumnuclear environment may be modified by different astrophysical processes over timescales longer than the accretion time near  $r_{acc}$ .

Finally, it must also be considered that the galactic ISM has a substantial and continuous mass input from stellar mass losses. A robust estimate for this source of mass is  $\dot{M}_{*} \simeq 1.5 \times 10^{-11} L_B(L_{\odot}) t(15\text{Gyr})^{-1.3} M_{\odot}\text{yr}^{-1}$  for an early-type galaxy of present blue luminosity  $L_B$  and age  $t$  (valid after an age of  $\sim 0.5$  Gyr; Ciotti et al. 1991); i.e.,  $\dot{M}_{*} \simeq 1.5 M_{\odot}\text{yr}^{-1}$  in a 15 Gyrs old galaxy of  $L_B = 10^{11} L_{\odot}$ . In stationary conditions (or quasi-stationary, since  $\dot{M}_{*}$  is a decreasing function of time  $t$ ) this  $\dot{M}_{*}$ , or a fraction of it coming from the inner few kpc of the galaxy, feeds a cooling flow towards the galactic center, if no strong heating

sources are present (e.g., Sarazin and White 1988; Pellegrini & Ciotti 1998). This has two consequences: 1) in the past the mass accretion rate towards the galactic center was likely higher than at the present epoch, since  $\dot{M}_*$  was higher; therefore in the past we may expect  $\dot{M}_B$  values higher than in Fig. 2, which constrains the duration of accretion phases to be even shorter; 2) for a low radiative efficiency scenario, where much less than  $\dot{M}_B$  can be accreted, to accommodate this continuous flow of mass towards  $r_{acc}$  (and the continuous mass source from within  $r_{acc}$  as well) may represent an additional problem. Again, feedback modulated accretion shows the advantage of efficiently removing gas from the galactic centers. This aspect of the intermittent scenario was in fact previously suggested as a solution for the well known problem of galactic cooling flows of accumulating too much cold gas at the galactic centers with respect to the observations, if lasting for many Gyrs.

In conclusion, the observational evidence provided by *Chandra* and the best estimates currently possible for the SMBH masses of nearby galactic nuclei show a large dispersion of the  $L_{X,nuc}$  and  $\dot{M}_B$  values, and lack of relationship between  $L_{X,nuc}$ ,  $M_{BH}$ ,  $\dot{M}_B$ , or their Eddington-scaled values, all quantities playing a fundamental role in accretion models. This seems to pose a challenge to models not providing feedback to the ISM, such as the Bondi accretion, ADAF and CDAF. Models with feedback may explain the observed scatter and also provide an efficient way of limiting the accumulation of mass towards the galactic centers predicted over cosmological times.

I thank G. Bertin for useful comments, L. Ciotti for discussions and D.W. Kim for information about his study on NGC1316. This work has been partially supported by MIUR (co-fin 2004).

## REFERENCES

- Baganoff, F. K., Bautz, M. W., Brandt, W. N., et al. 2001, *Nature*, 413, 45
- Baganoff, F. K., Maeda, Y., Morris, M., et al. 2003, *ApJ*, 591, 891
- Barth, A.J., Sarzi, M., Rix, H.W., Ho, L.C., Filippenko, A.V., & Sargent, W. L. W. 2001, *ApJ*, 555, 685
- Biller, B.A., Jones, C., Forman, W.R., Kraft, R., & Ensslin, T. 2004, *ApJ*, 613, 238
- Binney, J.J., & Tabor, G. 1995, *MNRAS*, 276, 663
- Blandford, R.D., & Begelman, M.C., 1999, *MNRAS*, 303, L1
- Blanton, E.L., Sarazin, C.L., & Irwin, J.A. 2001, *ApJ*, 552, 106
- Bondi, H. 1952, *MNRAS*, 112, 195
- Bower, G.A., et al. 1998, *ApJ*, 492, L111
- Cappellari, M., Verolme, E.K., van der Marel, R.P., Verdoes Kleijn, G.A., Illingworth, G.D., Franx, M., Carollo, C.M., & de Zeeuw, P.T. 2002, *ApJ*, 578, 787
- Ciotti, L., Pellegrini, S., Renzini, A., & D’Ercole, A. 1991, *ApJ*, 376, 380
- Ciotti, L., & Ostriker, J.P. 2001, *ApJ*, 551, 131
- Di Matteo, T., Allen, S.W., Fabian, A.C., Wilson, A.S., & Young, A.J. 2003, *ApJ*, 582, 133
- Elvis M. et al., 1994, *ApJS*, 95, 1
- Evans, D. A., Kraft, R. P., Worrall, D. M., Hardcastle, M. J., Jones, C., Forman, W. R., & Murray, S. S. 2004, *ApJ*, 612, 786
- Fabbiano, G., Elvis, M., Markoff, S., Siemiginowska, A., Pellegrini, S., Zezas, A., Nicastro, F., Trinchieri, G., & McDowell, J. 2003, *ApJ*, 588, 175
- Fabbiano, G., Baldi, A., Pellegrini, S., Siemiginowska, A., Elvis, M., Zezas, A., & McDowell, J. 2004, *ApJ*, 616, 730
- Faber, S. M., Tremaine, S., Ajhar, E.A., et al. 1997, *AJ*, 114, 1771
- Fabian, A.C., & Canizares, C.R. 1988, *Nature*, 333, 829
- Ferrarese, L., Ford, H.C., & Jaffe, W. 1996, *ApJ*, 470, 444

- Ferrarese, L., & Merritt, D. 2000, ApJ, 539, L9
- Filho, M. E., Fraternali, F., Markoff, S., Nagar, N. M., Barthel, P. D., Ho, L. C., & Yuan, F. 2004, A&A, 418, 429
- Finoguenov, A., & Jones, C. 2001, ApJ, 547, L10
- Frank, J., King, A., & Raine, D. 2002, *Accretion Power in Astrophysics*, Cambridge: CUP
- Gebhardt, K., Richstone, D., Ajhar, E.A., et al. 1996, AJ, 112, 105
- Gebhardt, K., Bender, R., Bower, G., et al. 2000, ApJ, 539, L13
- Gebhardt, K., Richstone, D., Tremaine, S., et al. 2003, ApJ, 583, 92
- Ghez, A.M., et al. 2003, ApJ, 586, L127
- Gliozzi, M., Sambruna, R. M., & Brandt, W.N. 2003, A&A, 408, 949
- Haiman, Z., Ciotti, L., & Ostriker, J. P. 2004, ApJ, 606, 763
- Ho, L.C., Filippenko, A. V., & Sargent, W.L. W. 1997, ApJ, 487, 568
- Ho, L. C. 1999, ApJ, 516, 672
- Ho, L. C. 2002, ApJ, 564, 120
- Ho, L.C., Feigelson, E.D., Townsley, L.K., et al. 2001, ApJ, 549, L51
- Ho, L. C., Terashima, Y., & Ulvestad, J.S. 2003, ApJ, 589, 783
- Humphrey, P.J., & Buote, D.A. 2004, ApJ, 612, 848
- Igumenshchev, I.V., Abramowicz, M.A., & Narayan, R. 2000, ApJ, 537, L27
- Irwin, J.A., Sarazin, C.L., & Bregman, J.N. 2002, ApJ, 570, 152
- Jeltema, T.E., Canizares, C.R., Buote, D.A., & Garmire, G.P. 2003, ApJ, 585, 756
- Kim, D. W., & Fabbiano, G. 2003, ApJ, 586, 826
- Kormendy, J., et al. 1996, ApJ, 473, L91
- Kraft, R.P., et al. 2003, ApJ, 592, 129
- Longo, G., Zaggia, S.R., Busarello, G., & Richter, G. 1994, A&AS, 105, 433

- Lowenstein, M., Mushotzky, R.F., Angelini, L., Arnaud, K.A., & Quataert, E. 2001, *ApJ*, 555, L21
- Macchetto, F., Marconi, A., Axon, D. J., Capetti, A., Sparks, W., & Crane, P. 1997, *ApJ*, 489, 579
- Machacek, M.E., Jones, C., & Forman, W.R. 2004, *ApJ*, 610, 183
- Magorrian, J., et al. 1998, *AJ*, 115, 2285
- Marconi, A., Capetti, A., Axon, D.J., Koekemoer, A., Macchetto, D., & Schreier, E.J. 2001, *ApJ*, 549, 915
- McElroy, D.B. 1995, *ApJS*, 100, 105
- Mei, S., Silva, D., & Quinn, P.J. 2000, *A&A*, 361, 68
- Narayan, R., & Yi, I. 1995, *ApJ*, 444, 231
- Ohto, A., Kawano, N., & Fukazawa, Y. 2003, *PASJ*, 55, 819
- Omma, H., Binney, J., Bryan, G., & Slyz, A. 2004, *MNRAS*, 348, 1105
- Pellegrini, S., & Ciotti, L. 1998, *A&A*333, 433.
- Pellegrini, S., Baldi, A., Fabbiano, G., & Kim, D.W. 2003a, *ApJ*, 597, 175
- Pellegrini, S., Venturi, T., Comastri, A., Fabbiano, G., Fiore, F., Vignali, C., Morganti, R., & Trinchieri, G. 2003b, *ApJ*, 585, 677
- Phillips M.M., Jenkins C.R., Dopita M.A., Sadler E.M., Binette L., 1986, *AJ*, 91,1062
- Proga, D., Begelman, M.C. 2003, *ApJ*, 582, 69
- Quataert, E. 2003, *Astronomische Nachrichten*, vol. 324, Suppl. Issue 1, p. 435.
- Quataert, E., & Gruzinov, A. 2000, *ApJ*, 539, 809
- Richstone, D., et al 1998, *Nature*, 395, 14
- Satyapal, S., Sambruna, R. M., & Dudik, R. P. 2004, *A&A*, 414, 825
- Sarazin, C.L., & White, R.E. III 1988, *ApJ*, 331, 102
- Sarazin, C. L., Irwin, J.A., & Bregman, J.N. 2001, *ApJ*, 556, 533

- Shakura, N.J., & Sunyaev, R.A. 1973, *A&A*, 24, 337
- Sivakoff, G.R., Sarazin, C.L., & Irwin, J.A. 2003, *ApJ*, 599, 218
- Sivakoff, G.R., Sarazin, C.L., & Carlin, J.L. 2004, *ApJ*, 617, 262
- Schödel, R., Ott, T., Genzel, R., Eckart, A., Mouawad, N., & Alexander, T. 2003, *ApJ*, 596, 1015
- Soldatenkov, D. A., Vikhlinin, A. A., & Pavlinsky, M. N. 2003, *AstL*, 29, 298
- Soria, R., et al. 2005, in preparation
- Terashima, Y., & Wilson, A. S. 2004, *ApJ*583, 145
- Tonry, J.L., Dressler, A., Blakeslee, J.P., et al. 2001, *ApJ*, 546, 681
- Tremaine, S., Gebhardt, K., Bender, R., et al. 2002, *ApJ*, 574, 740
- van der Marel, R.P. 1999, *AJ*, 117, 744
- Van Speybroeck, L. P., Jerius, D., Edgar, R. J., Gaetz T. J., & Zhao, P. 1997, *Proc. SPIE*, 3113, 89
- Verolme, E. K., Cappellari, M., Copin, Y., et al. 2002, *MNRAS*, 335, 517
- Wills, K.A., Tadhunter, C.N., Robinson, T.G., Morganti, R., 2002, *MNRAS*, 333, 211
- Yi, I., & Boughn, S. P. 1999, *ApJ*, 515, 576
- Yu, Q., & Tremaine, S. 2002, *MNRAS*, 335, 965
- Yuan, F., Peng, Q., Lu, J., Wang, J. 2000, *ApJ*, 537, 236
- Yuan, F., Quataert, E., & Narayan, R. 2003, *ApJ*598, 301
- Zhang, Z.-Li, & Xu, H. 2004, *ChJAA* 4, 221

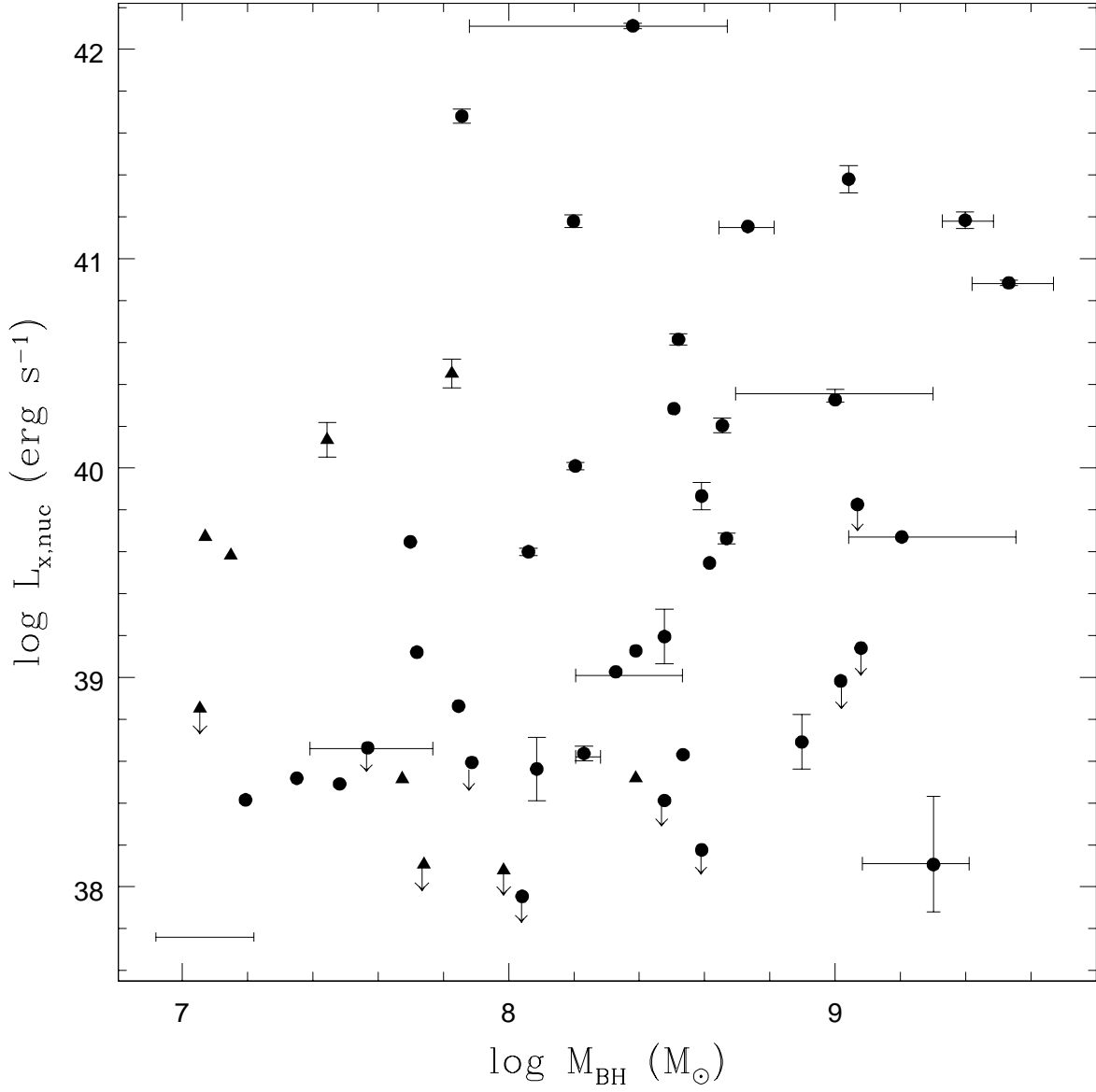


Fig. 1.— The relation between the nuclear X-ray luminosity, as measured from *Chandra* data, and the central SMBH mass, for the galaxies in Table 1 (see Sect. 3.1). Circles indicate morphological types from E to Sa included, triangles the other types (i.e., from Sab to Sbc). Arrows indicate upper limits on  $L_{X,nuc}$ ; uncertainties on  $L_{X,nuc}$  are shown as errorbars when derivable from the literature. The uncertainties on  $M_{BH}$  are also shown as errorbars;  $M_{BH}$  values estimated from the  $M_{BH} - \sigma$  relation have an uncertainty plotted in the lower left corner (Tremaine et al. 2002). M32 and the Galactic Center do not appear in this plot since their  $L_{X,nuc}$  is too low by orders of magnitude (Tab. 1).

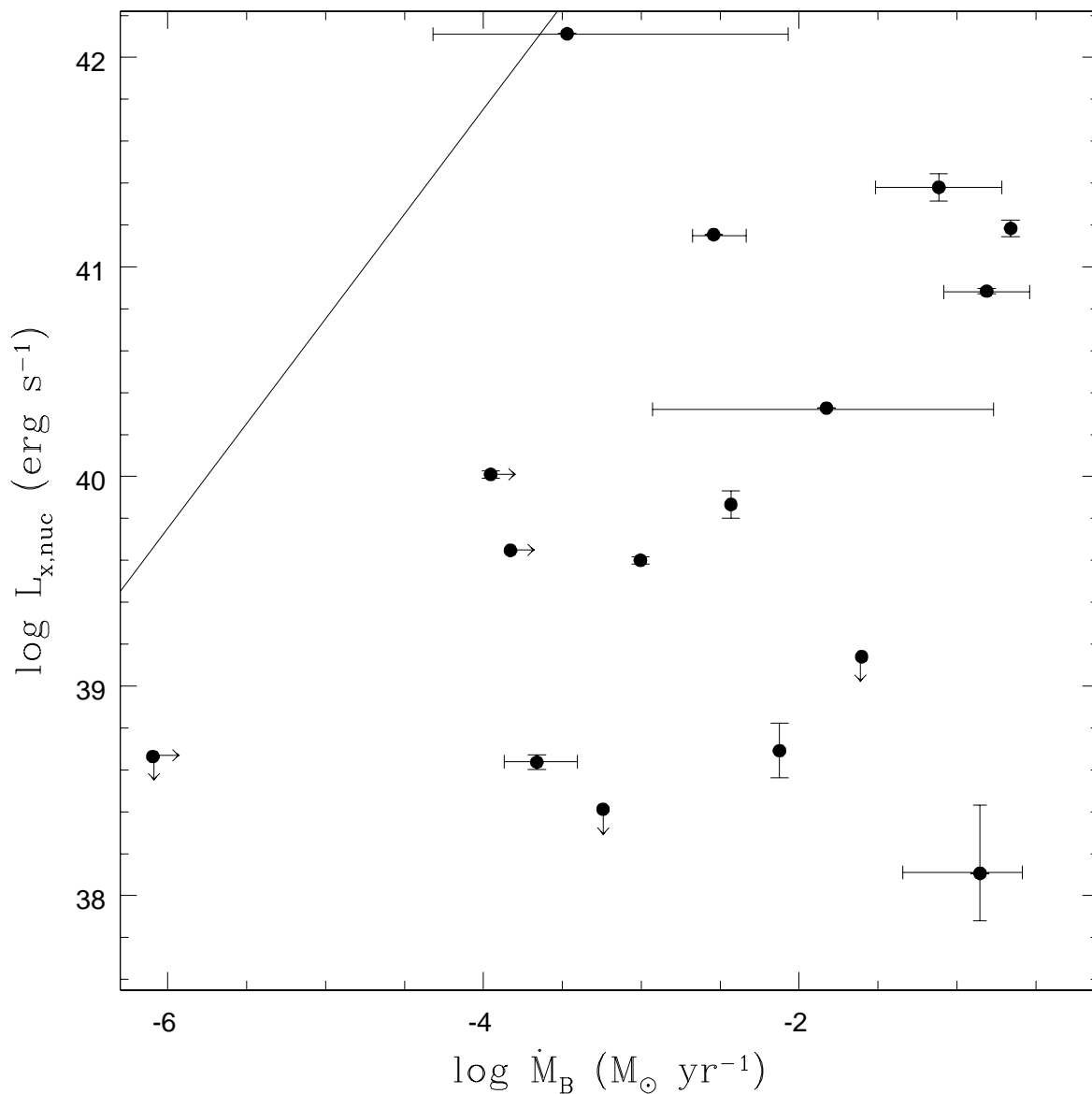


Fig. 2.— The relation between  $L_{X,nuc}$  and the Bondi mass accretion rate  $\dot{M}_B$  estimated as described in Sect. 3.2. Downward arrows and errorbars on  $L_{X,nuc}$  are as for Fig. 1. Rightward arrows indicate underestimates of  $\dot{M}_B$  and errorbars its uncertainty, calculated as described in Sect. 3.2. The solid line represents  $L_{acc} = 0.1\dot{M}_B c^2$  (Sect. 3.3). As for Fig. 1, M32 and the Galactic Center cannot appear in the plot.



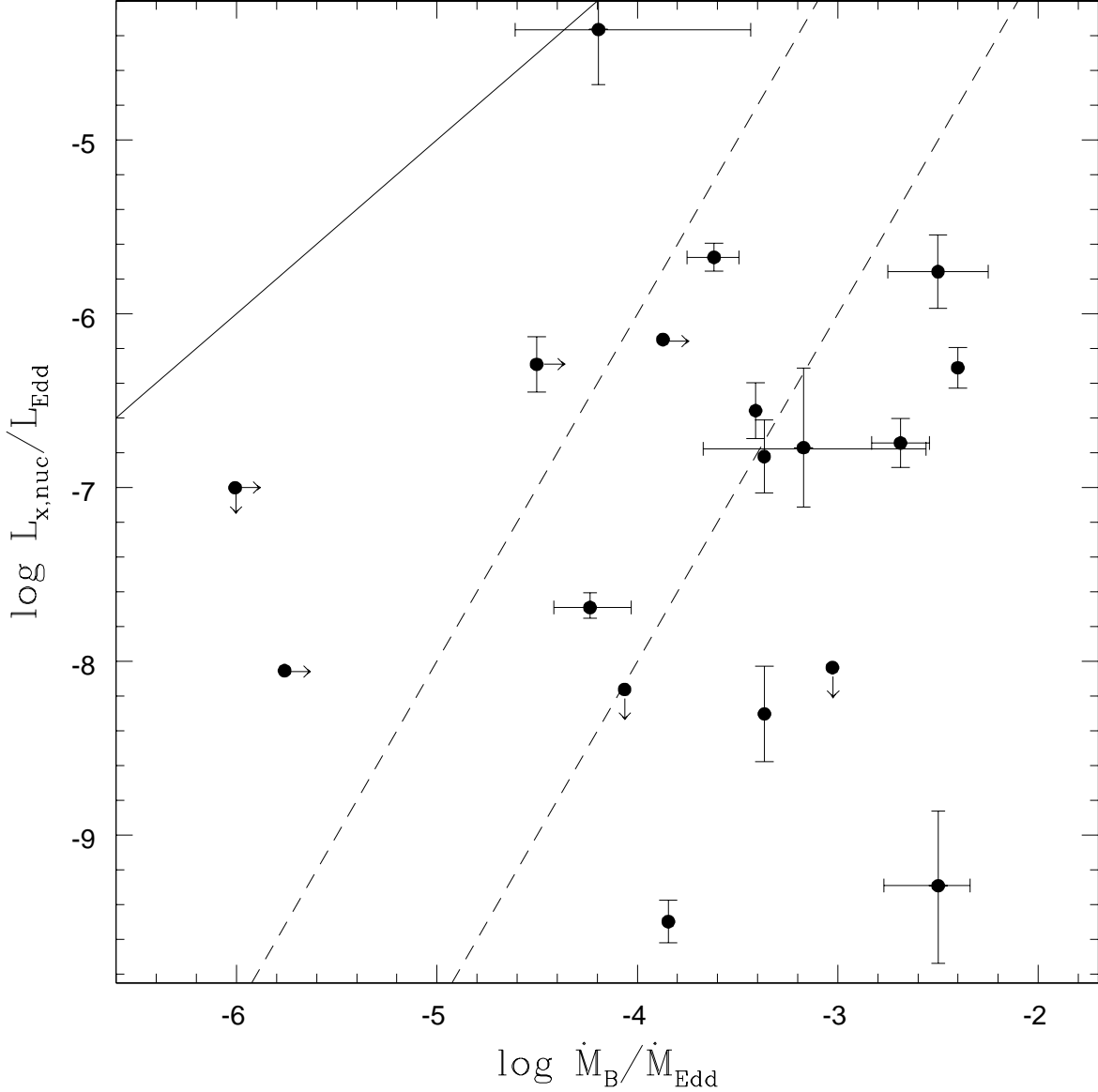


Fig. 3.— The relation between  $L_{X,nuc}$  scaled by the Eddington luminosity and  $\dot{M}_B$  scaled by the Eddington mass accretion rate. The solid line indicates  $L_{acc}/L_{Edd}$ ; the dashed lines indicate  $L_{ADAF}/L_{Edd}$ , the expected emission level for a standard ADAF model with  $\dot{M} = \dot{M}_B$  or  $\dot{M} = \alpha \dot{M}_B$  and  $\alpha = 0.1$  (see Sect. 3.4). The other symbols are the same as for Fig. 2. The Galactic Center is the point with the lowest  $L_{X,nuc}/L_{Edd}$ , and in this case its  $L_{X,nuc}$  corresponds to its strongest flare (Baganoff et al. 2001, converted to the 0.3–10 keV band).

Table 1. The sample

Galaxy	D	$M_{BH}$	Ref.	$kT$	$\rho$	$\log L_{X,nuc}^a$	Ref.
(1)	(Mpc)	( $10^8 M_{\odot}$ )	(4)	(keV)	( $10^{-24} \text{g cm}^{-3}$ )	( $\text{erg s}^{-1}$ )	(8)
(1)	(2)	(3)	(4)	(5)	(6)	(7)	(8)
NGC221 (M32)	0.81	$0.025 \pm 0.005$	1	$0.37^{+0.28}_{-0.19}$	0.13	36.44	1
NGC821	24.1	$0.37^{+0.17}_{-0.15}$	2	$0.46^{+0.33}_{-0.25}$	$0.01^{+0.027}_{-0.004}$	<38.66	2
NGC1291	8.9 <sup>b</sup>	1.1	3	0.34	0.56	39.60	3
NGC1316	21.5	3.9	3	$0.62 \pm 0.02$	0.44	39.87	4
NGC1399	20.0	12	3	0.8	0.47	<39.14	5
NGC1553	18.5	1.6	3	$0.51^{+0.07}_{-0.08}$	0.06	40.01	6
NGC4261	31.6	$5.4 \pm 1.1$	4	$0.6 \pm 0.02$	$0.17 \pm 0.01$	41.15	7
NGC4438	16.1	0.5	5	$0.58^{+0.04}_{-0.10}$	0.99	39.65	8
NGC4472	16.3	7.9	3	0.8	0.32	38.69	5,9 <sup>c</sup>
NGC4486 (M87)	16.1	$34 \pm 10$	6	$0.8 \pm 0.01$	$0.36 \pm 0.006$	40.88	10
NGC4594 (Sombrero)	9.8	$10^{+10}_{-7}$	7	$0.65^{+0.05}_{-0.35}$	$0.29 \pm 0.10$	40.34	11
NGC4636	14.7	3.0	3	0.6	0.11	<38.41	5
NGC4649	16.8	$20^{+5}_{-10}$	2	$0.86 \pm 0.02$	$1.05 \pm 0.1$	38.11	12
NGC4697	11.7	$1.7^{+0.2}_{-0.1}$	2	$0.33^{+0.06}_{-0.04}$	$0.05 \pm 0.01$	38.64	13
NGC5128 (Cen A)	4.2	$2.4^{+3.6}_{-1.7}$	8	$0.50 \pm 0.05$	$0.08 \pm 0.01$	42.11	14
IC1459	29.2	$25^{+5}_{-4}$	9	$0.5 \pm 0.1$	0.54	41.18	15
IC4296	49 <sup>d</sup>	11.	3	$0.56 \pm 0.03$	$1.0 \pm 0.17$	41.38	16
NGC660	11.8 <sup>e</sup>	0.22	3	–	–	38.52	17
NGC720	27.7	3.0	3	–	–	39.19	18
NGC1332	22.9	10	3	–	–	<38.98	19
NGC1407	28.8	4.6	3	–	–	39.66	20
NGC1600	60 <sup>e</sup>	12.	3	–	–	<39.83	21
NGC2787	7.48	1.2	3	–	–	38.56	22
NGC2841	12.0 <sup>e</sup>	2.4	3	–	–	38.52	23
NGC3169	19.7 <sup>e</sup>	0.7	3	–	–	41.68	22
NGC3226	23.6	1.6	3	–	–	41.18	22
NGC3245	20.9	$2.13^{+1.0}_{-0.6}$	10	–	–	39.03	17
NGC3368	10.4	0.14	3	–	–	39.58	24
NGC3489	12.1	0.30	3	–	–	38.49	23
NGC3623	10.8 <sup>e</sup>	0.70	3	–	–	38.86	24
NGC3627	6.6 <sup>e</sup>	0.97	3	–	–	<38.08	17
NGC4125	23.9	2.4	3	–	–	39.13	24
NGC4143	15.9	4.5	3	–	–	40.20	22
NGC4278	16.1	3.3	3	–	–	40.61	22
NGC4314	12.8 <sup>e</sup>	0.16	3	–	–	38.41	24
NGC4321	16.1 <sup>e</sup>	0.11	3	–	–	<38.85	23
NGC4365	20.4	3.9	3	–	–	<38.18	25
NGC4374	18.4	$16^{+20}_{-6}$	11	–	–	39.67	26
NGC4382	18.5	1.1	3	–	–	<37.95	25
NGC4494	17.1	0.52	3	–	–	39.12	23
NGC4548	19.2	0.28	3	–	–	40.13	22
NGC4552	15.4	4.1	3	–	–	39.55	17
NGC4569	16.8 <sup>e</sup>	0.12	3	–	–	39.67	23
NGC4696	35.5	3.2	3	–	–	40.28	24

Table 1—Continued

Galaxy	D	$M_{BH}$	Ref.	$kT$	$\rho$	$\log L_{X,nuc}^a$	Ref.
(1)	(Mpc)	( $10^8 M_{\odot}$ )	(4)	(keV)	( $10^{-24} \text{g cm}^{-3}$ )	( $\text{erg s}^{-1}$ )	(8)
(1)	(2)	(3)	(4)	(5)	(6)	(7)	(8)
NGC4826	7.5	0.55	3	–	–	<38.11	23
NGC5846	24.9	3.4	3	–	–	38.63	17
NGC5866	15.3	0.77	3	–	–	<38.59	22
NGC6500	39.7 <sup>e</sup>	0.67	3	–	–	40.45	22
NGC7331	13.1	0.47	3	–	–	38.51	22
Milky Way	0.008	0.034±0.005	12	1.3	52.	33.38	27

<sup>a</sup>Nuclear X-ray luminosities refer to the 0.3–10 keV band; if they were derived in a different band by the authors in column 8, they have been converted to 0.3–10 keV by using the spectral shape adopted by these authors.

<sup>b</sup>The adopted distance is that of the X-ray analysis paper.

<sup>c</sup> $kT$  and  $\rho$  have been estimated by Ref. 5, while  $L_{X,nuc}$  of Ref. 9 has been adopted.

<sup>d</sup>This distance has been derived with the SBF method by Mei et al. 2000.

<sup>e</sup>The adopted distance refers to  $H_0 = 75 \text{ km s}^{-1} \text{ Mpc}^{-1}$ .

References. — for column 4: (1) Verolme et al. 2002; (2) Gebhardt et al. 2003; (3)  $M_{BH}$  derives from the  $M_{BH} - \sigma$  relation of Tremaine et al. 2002, with  $\sigma$  from McElroy 1995, except for NGC1553, for which  $\sigma = 186 \text{ km s}^{-1}$  (Longo et al. 1994); (4) Ferrarese et al. 1996; (5) Machacek et al. 2004; (6) Macchetto et al. 1997; (7) Kormendy et al. 1996; (8) Marconi et al. 2001; (9) Cappellari et al. 2002; (10) Barth et al. 2001; (11) Bower et al. 1998; (12) Schödel et al. 2003.

References. — for column 8: (1) Ho et al. 2003; (2) Fabbiano et al. 2004; (3) Irwin et al. 2002; (4) Kim & Fabbiano 2003; (5) Loewenstein et al. 2001; (6) Blanton et al. 2001; (7) Gliozzi et al. 2003; (8) Machacek et al. 2004; (9) Biller et al. 2004; (10) Di Matteo et al. 2003; (11) Pellegrini et al. 2003a; (12) Soldatenkov et al. 2003; (13) Soria et al. (2005) and Sarazin et al. 2001; (14) Evans et al. 2004 and Kraft et al. (2003); (15) Fabbiano et al. 2003; (16) Pellegrini et al. 2003b; (17) Filho et al. 2004; (18) Jeltama et al. 2003; (19) Humphrey & Buote 2004; (20) Zhang & Xu 2004; (21) Sivakoff et al. 2004; (22) Terashima & Wilson 2003; (23) Ho et al. 2001; (24) Satyapal et al. 2004; (25) Sivakoff et al. 2003; (26) Finoguenov & Jones 2001; (27) Baganoff et al. (2003; the X-ray luminosity refers to the quiescent state, for the 2–10 keV band).